

Structure, Thermal Stability and Mechanical Properties of $\text{Zr}_{65}\text{Al}_{7.5}\text{Ni}_{10}\text{Cu}_{17.5}$ Glassy Alloy Rod with a Diameter of 16 mm Produced by Tilt Casting

Q. S. Zhang¹, W. Zhang^{1,*}, X. M. Wang¹, Y. Yokoyama¹, K. Yubuta¹ and A. Inoue²

¹Institute for Materials Research, Tohoku University, Sendai 980-8577, Japan

²WPI, Advanced Institute for Materials Research, Tohoku University, Sendai 980-8577, Japan

Bulk glassy alloy rods with a diameter of 16 mm and a length of 40 to 45 mm were produced for $\text{Zr}_{65}\text{Al}_{7.5}\text{Ni}_{10}\text{Cu}_{17.5}$ alloy by a tilt casting method. The alloy specimens taken from the different sites which are away by about 10 mm, 15 mm and 30 mm from the bottom surface of the cast rod consist of a glassy phase and their thermal stability, mechanical properties and fracture mode are almost independent of the specimen sites. The glass transition temperature, temperature interval of supercooled liquid region before crystallization and heat of crystallization are about 643 K, 102 K and 55 J/g, respectively, for the specimens taken from the three different sites. Besides, Young's modulus, yield strength, fracture strength, yield strain and plastic strain of the specimens are about 87 GPa, 1540 MPa, 1580 MPa, 0.018 and 0.005, respectively. The fracture mode consisting of shear plastic deformation along the maximum shear stress plane, followed by an instantaneous final rupture is also independent of the specimen sites. These data indicate that the cast glassy alloy rod with a diameter of 16 mm has nearly the same characteristics, though the cooling rate is significantly dependent on sample sites. The knowledge of producing the Zr-based bulk glassy alloy rod with nearly the same characteristics in the large diameter range up to 16 mm is encouraging for future applications of bulk glassy alloys as a new type of engineering material. [doi:10.2320/matertrans.MER2008127]

(Received April 10, 2008; Accepted June 19, 2008; Published August 25, 2008)

Keywords: bulk glassy alloy, mechanical property, thermal stability, Zr-based alloy, tilt casting

1. Introduction

For the past two decades, much attention has been paid to bulk glassy alloys because of their scientific and engineering novelties. The trigger of active researches on bulk glassy alloy fields has been attributed to the findings of multi-component glassy alloys in Mg-,¹⁾ lanthanide (Ln)-²⁾ and Zr-³⁾ based alloy systems exhibiting a large supercooled liquid region before crystallization which had been achieved for several years between 1988 and 1992. Subsequently, bulk glassy alloys with thicknesses of larger than several millimeters were produced by conventional casting methods on the basis of high stabilization of supercooled liquid against crystallization.⁴⁻⁷⁾ It was subsequently proposed in 1994 that their bulk glassy alloys had following unique three features of alloy components,⁸⁾ i.e., (1) multi-component alloy system consisting of more than three elements, (2) significant atomic size mismatches above 12% among their main three constituent elements, and (3) negative heats of mixing among the main three elements. It is well known that a number of bulk glassy alloy systems such as Ti-, Fe-, Pd-Cu-, Co-, Ni-, Pt- and Cu-based alloys have been developed on the basis of the three component rules for the past 15 years.^{9,10)} When we focus on Zr-based bulk glassy alloys containing Zr contents more than 50 at%, their basic alloy systems are limited to Zr-Al-Ni,³⁾ Zr-Al-Cu,¹¹⁾ Zr-Al-Ni-Cu^{7,12)} and Zr-Al-Ni-Cu-TM (TM = Ti, Hf, Nb, Pd, Pt, Ag, Au)¹³⁾ systems. In 1993, the formation of glassy phase in coexistence with crystalline phase in $\text{Zr}_{65}\text{Al}_{7.5}\text{Ni}_{10}\text{Cu}_{17.5}$ alloy has been reported in the rod specimen with a diameter of 16 mm prepared by liquid quenching the alloy melt in a quartz tube.⁷⁾ However, the melting method in quartz tube for the formation of Zr-rich bulk glassy alloys with diameters above 10 mm has not been used at present because of the recognition of significant

harmful reaction between quartz tube and reactive Zr-based alloy liquid. For the past 15 years, it is noticed that the dissolution of oxygen and silicon elements and the mixture of SiO_2 cause harmful influence on the glass-forming ability of Zr-based alloys through preferential nucleation and growth reactions caused by SiO_2 as well as the reduction of glass-forming ability due to the dissolution of their elements.¹⁴⁻¹⁶⁾ Considering the previous production process using the melting method in quartz tube for $\text{Zr}_{65}\text{Al}_{7.5}\text{Ni}_{10}\text{Cu}_{17.5}$ alloy, little is known about a true critical diameter for formation of a bulk glassy alloy at the Zr-rich composition. Besides, there have been no definite data on the compositional dependence of maximum diameter for glass formation for Zr-Al-Ni-Cu system, though the largest diameter of 30 mm has been obtained for $\text{Zr}_{55}\text{Al}_{10}\text{Ni}_5\text{Cu}_{30}$ with a much lower Zr concentration by suction casting¹²⁾ and cap casting¹⁷⁾ methods. We have examined a maximum diameter of $\text{Zr}_{65}\text{Al}_{7.5}\text{Ni}_{10}\text{Cu}_{17.5}$ glassy alloy produced by tilt casting¹⁸⁾ which can be regarded as a kind of conventional copper mold casting methods and noticed that the maximum diameter for formation of glassy phase reaches at least 16 mm. This paper intends to present the formation, thermal stability and mechanical properties of the Zr-Al-Ni-Cu bulk glassy alloy rod with a diameter of 16 mm and to discuss the importance of the bulk glassy alloy as an engineering material with high strength and highly ductile nature.

2. Experimental Procedure

An alloy ingot with composition of $\text{Zr}_{65}\text{Al}_{7.5}\text{Ni}_{10}\text{Cu}_{17.5}$ was prepared by arc melting the mixture of pure metals with purity of 99.9 mass% for Zr and 99.99 mass% for Al, Ni and Cu in an argon atmosphere. The alloy composition represents nominal atomic percentage. Bulk glassy alloy rods of 16 mm in diameter and about 45 mm in length were prepared from the pre-alloyed ingot by using a tilt casting method using a

*Corresponding author, E-mail: wzhang@imr.tohoku.ac.jp

copper mold in an argon atmosphere. The glassy structure of the cast alloy rods was identified by X-ray diffraction, optical microscopy (OM) and transmission electron microscopy (TEM). The etching for OM observation specimen was made in a 0.5% aqueous fluoride acid solution for 5 s at 298 K. The TEM specimen was made by electrical polishing, followed by a low energy ion milling treatment. The thermal stability associated with glass transition, supercooled liquid region and crystallization was examined by differential scanning calorimetry (DSC) at a heating rate of 0.67 K s^{-1} . The liquidus and melting temperatures were also measured by differential thermal analyzer (DTA) at heating and cooling rates of 0.33 K s^{-1} . Mechanical properties under a compressive applied load were measured by using an Instron testing machine. The gauge dimension for the mechanical test specimen was $2 \times 2 \times 4 \text{ mm}^3$ and its strain rate was fixed as $5.0 \times 10^{-4} \text{ s}^{-1}$. Deformation shear band and fracture morphology were examined by scanning electron microscopy (SEM).

3. Results

3.1 Glass formation

Figure 1 shows outer shape and surface morphology of a $\text{Zr}_{65}\text{Al}_{7.5}\text{Ni}_{10}\text{Cu}_{17.5}$ alloy rod with a diameter of 16 mm produced by the tilt casting method. The alloy rod exhibits smooth outer surface with good metallic luster and no distinct surface ruggedness due to the precipitation of a crystalline phase is observed. With the aim of confirming the absence of crystalline phase in the glassy alloy rod, the cross sectional structure was examined by optical microscopy, X-ray diffraction and high resolution TEM technique. Figure 2 shows optical micrographs of the central region in the transverse cross sections at different sites which are away by about 10 mm, 15 mm and 30 mm from the bottom surface of the cast alloy rod with a diameter of 16 mm. The sites for OM observation specimens are illustrated in Fig. 3, where the sites for the specimens for X-ray diffraction, TEM observation, DSC, mechanical properties and fracture mode are also shown. Even after the etching treatment, no appreciable



Fig. 1 Outer shape and surface morphology of $\text{Zr}_{65}\text{Al}_{7.5}\text{Ni}_{10}\text{Cu}_{17.5}$ alloy rod with a diameter of 16 mm and a length of about 45 mm produced by the tilt casting method.

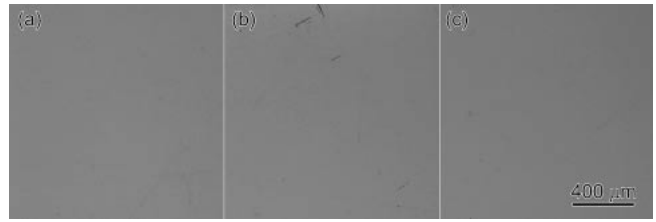


Fig. 2 Optical micrographs of the central region in the transverse cross section taken from the sites which are away by 10 mm (a), 15 mm (b) and 30 mm (c) from the bottom surface of the cast $\text{Zr}_{65}\text{Al}_{7.5}\text{Ni}_{10}\text{Cu}_{17.5}$ alloy rod with a diameter of 16 mm.

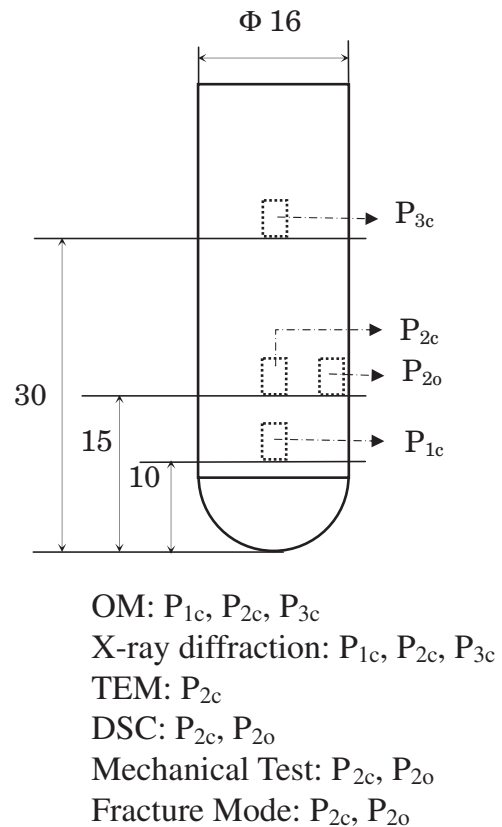


Fig. 3 Schematic illustration showing the preparation sites of the samples used for various characterizations and measurements in the cast $\text{Zr}_{65}\text{Al}_{7.5}\text{Ni}_{10}\text{Cu}_{17.5}$ alloy rod with a diameter of 16 mm.

contrast due to the precipitation of crystalline phases is seen over the whole cross sections of the different sites for the alloy ingot. In addition, Fig. 4 shows X-ray diffraction patterns of the central region in the transverse cross sections at different sites which are away by about 10 mm, 15 mm and 30 mm from the bottom surface of the cast alloy rod with a diameter of 16 mm. All the X-ray diffraction patterns consist of broad peaks and no distinct sharp peak due to the existence of a crystalline phase is recognized. We also tried to confirm the absence of any crystalline phase on the basis of high resolution TEM images. As exemplified in Fig. 5(a) and (b), the high resolution TEM images taken from the central region in the transverse cross section which is about 15 mm away from the bottom surface reveal only a modulated contrast typical for a glassy single phase and neither medium-range ordered atomic configurations nor nanoscale crystal-

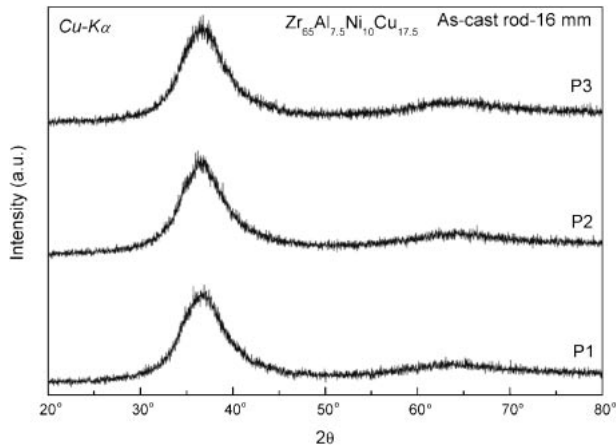


Fig. 4 X-ray diffraction patterns of their corresponding regions shown in Fig. 2.

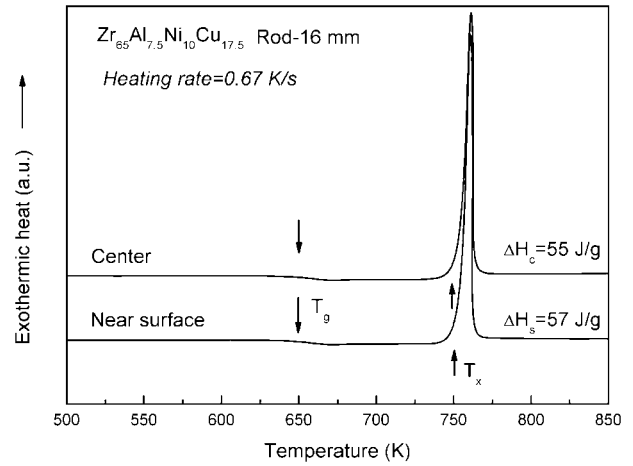


Fig. 6 DSC curves of the central and surface regions in the transverse cross section taken from the site which is about 15 mm away from the bottom surface of the cast $\text{Zr}_{65}\text{Al}_{7.5}\text{Ni}_{10}\text{Cu}_{17.5}$ alloy rod with a diameter of 16 mm.

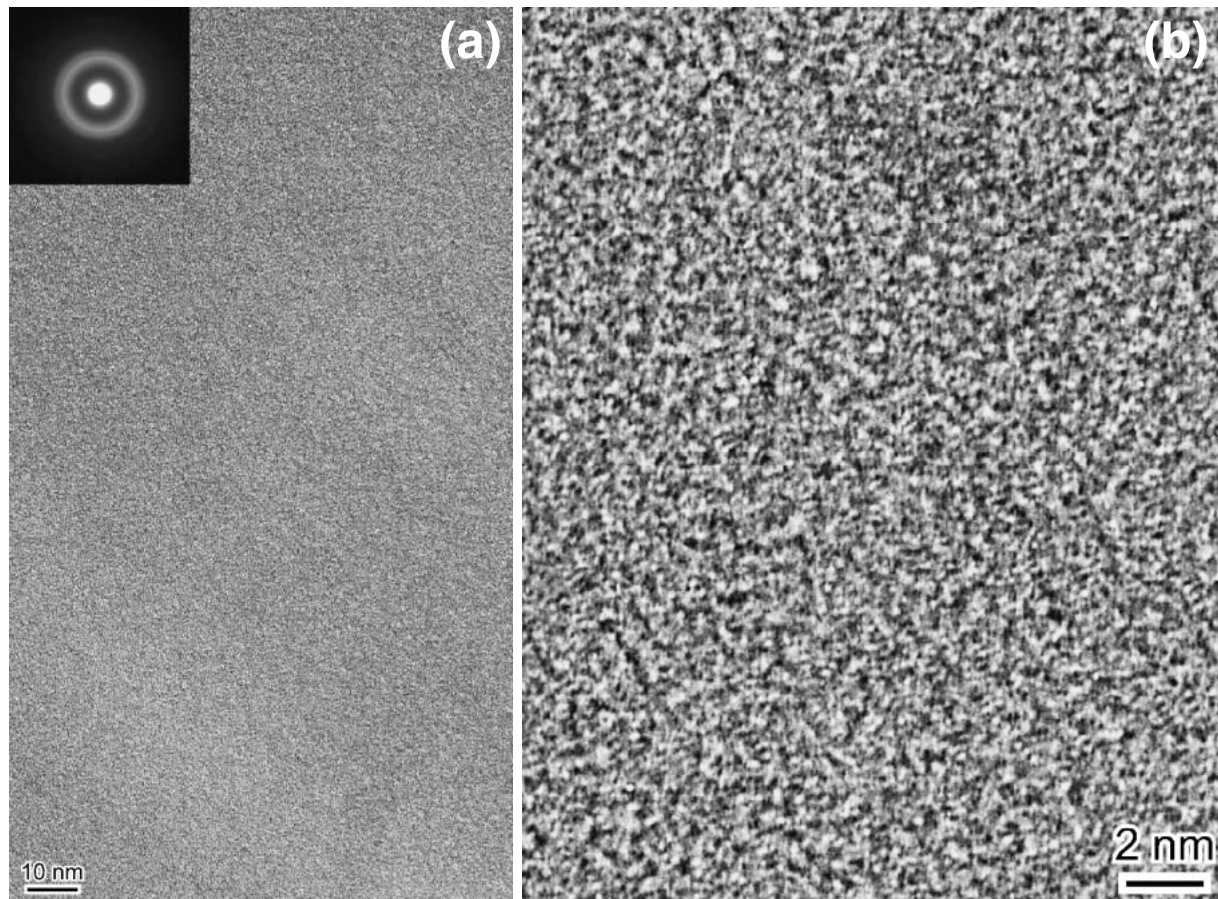


Fig. 5 High resolution electron micrographs and selected area electron diffraction pattern of the central region in the transverse cross section taken from the site which is about 15 mm away from the bottom surface of the cast $\text{Zr}_{65}\text{Al}_{7.5}\text{Ni}_{10}\text{Cu}_{17.5}$ alloy rod with a diameter of 16 mm.

line phase are observed. Besides, the selected-area electron diffraction pattern also consists of only halo rings, indicating the formation of a glassy single phase. These metallographic results indicate that the alloy rod is composed of a glassy phase and the formation tendency of the glassy phase is independent of the site in the cast alloy rod. It is thus

concluded that the $\text{Zr}_{65}\text{Al}_{7.5}\text{Ni}_{10}\text{Cu}_{17.5}$ alloy has the critical diameter of at least 16 mm.

3.2 Thermal stability

Figure 6 shows DSC curves of the central and outer surface regions in the transverse cross section at the site

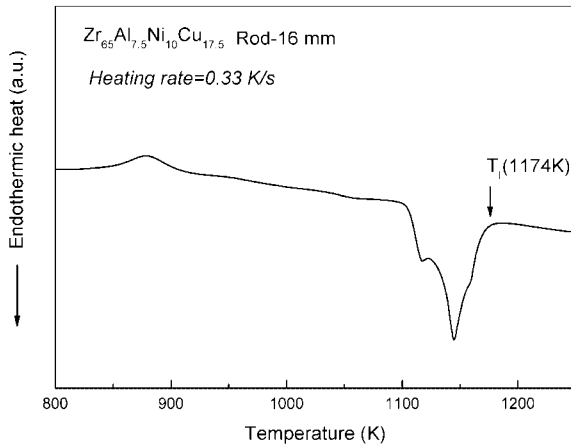


Fig. 7 DTA curve of the cast $\text{Zr}_{65}\text{Al}_{7.5}\text{Ni}_{10}\text{Cu}_{17.5}$ glassy alloy rod with a diameter of 16 mm.

which is about 15 mm away from the bottom surface of the alloy rod. One can see a distinct endothermic reaction due to glass transition at 643 K (T_g), followed by a supercooled liquid region with a temperature interval of 102 K ($\Delta T_x = T_x - T_g$) and then a sharp exothermic peak at the onset temperature of 745 K (T_x) due to crystallization. Thus, no distinct difference in T_g , ΔT_x , T_x and ΔH_x between the central region and outer surface region is recognized on the DSC curves. The heat of crystallization (ΔH_x) was measured to be 55 J/g at the central region and 57 J/g at the outer surface region. We also measured the liquidus temperature of the cast glassy alloy rod with a diameter of 16 mm by DTA. As shown in Fig. 7, the melting appears to occur through three stages and is completed at 1174 K. The three stages overlap with each other within a temperature interval of about 75 K, indicating that the present quaternary alloy is located near multi-component eutectic point. Based on the data of T_g and T_1 , the reduced glass transition temperature (T_g/T_1) is evaluated to be as high as 0.55, indicating that the Zr-based alloy has high glass-forming ability.

3.3 Mechanical Properties

Figure 8 shows compressive stress-strain curves of the cast $\text{Zr}_{65}\text{Al}_{7.5}\text{Ni}_{10}\text{Cu}_{17.5}$ alloy rod with a diameter of 16 mm. The test specimens were taken from the central and outer surface regions in the transverse cross section at the fixed site which is about 15 mm away from the bottom surface of the alloy rod. The alloy exhibits elastic deformation with a strain up to about 0.018, followed by plastic strains of about 0.003 at the central region and 0.005 at the outer surface region accompanying serration pattern, and then final rupture. The Young's modulus and yield strength are estimated to be 88 GPa and 1540 MPa, respectively, at the central region and 85 GPa and 1550 MPa, respectively, at the outer surface region. Thus, the mechanical strength appears to be independent of the sample site in the transverse cross section. Figure 9 shows fracture morphology and fracture surface appearance of the central and outer surface regions. Both the samples fracture along the maximum shear stress plane which is declined by about 45 degrees to the direction of applied load and the fracture surface consists of mainly a well

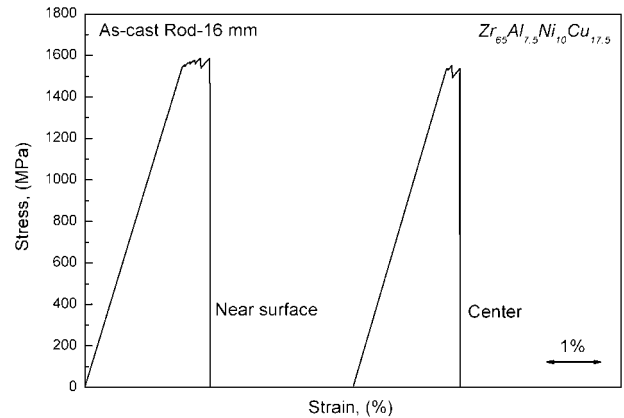


Fig. 8 Compressive stress-strain curves of the alloy specimens taken from the central and surface regions in the transverse cross section taken from the site which is about 15 mm away from the bottom surface of the cast $\text{Zr}_{65}\text{Al}_{7.5}\text{Ni}_{10}\text{Cu}_{17.5}$ alloy rod with a diameter of 16 mm.

developed vein pattern. In addition, one can see a number of shear bands on the lateral surface near the fracture site, being consistent with the generation of serrated plastic flow before final rupture.

4. Discussion

All the data in the present paper demonstrate clearly that the $\text{Zr}_{65}\text{Al}_{7.5}\text{Ni}_{10}\text{Cu}_{17.5}$ alloy has high glass-forming ability leading to the formation of bulk glassy alloy rods with diameters up to 16 mm by the tilt casting method¹⁸⁾ which can be regarded as the conventional copper mold casting process. Although a number of bulk glassy alloys with diameters above 16 mm have been reported in metal-metal type alloys, the bulk glassy alloys except $\text{Zr}_{65}\text{Al}_{7.5}\text{Ni}_{10}\text{Cu}_{17.5}$ include large amounts (about 45 to 60 at%) of solute elements, as exemplified for $\text{Zr}_{55}\text{Al}_{10}\text{Ni}_5\text{Cu}_{30}$,^{12,18)} $\text{Zr}_{41.2}\text{Be}_{22.5}\text{Ti}_{13.8}\text{-Cu}_{12.5}\text{Ni}_{10}$,¹⁹⁾ $\text{Zr}_{48}\text{Al}_8\text{Cu}_{36}\text{Ag}_8$ ²⁰⁾ and $\text{Zr}_{48}\text{Al}_8\text{Cu}_{34}\text{Ag}_8\text{Pd}_2$.²¹⁾ Thus, the present $\text{Zr}_{65}\text{Al}_{7.5}\text{Ni}_{10}\text{Cu}_{17.5}$ alloy has the lowest solute content among the Zr-based bulk glassy alloys with large critical diameters above 15 mm. Very recently, it has been found^{22–24)} that Zr-based bulk glassy alloys with low solute contents ranging from 30 to 40 at% in Zr-Al-Cu and Zr-Al-Ni-Cu systems exhibit improved characteristics in compressive ductility, Charpy impact fracture energy, fracture toughness and fatigue strength in as-cast and annealed states. Thus, it is important to clarify the possibility of forming a bulk glassy alloy with large critical diameter for Zr-based alloys containing low solute contents less than 40 at%, because reliable mechanical properties are the most important for applications to structural materials.

Besides, it is presumed that the reason for the high glass-forming ability of the Zr-rich bulk glassy alloy with the low solute content of 35 at% is different from that for the bulk glassy alloys with high solute contents exceeding 50 at%. The high glass-forming ability of the $\text{Zr}_{65}\text{Al}_{7.5}\text{Ni}_{10}\text{Cu}_{17.5}$ glassy alloy seems to result from the combination of a large supercooled liquid region of 102 K, a rather high T_g/T_1 of 0.55 and the composition near the multi-component eutectic point as is evidenced from the overlap of three melting (endothermic) stages within a relatively narrow temperature

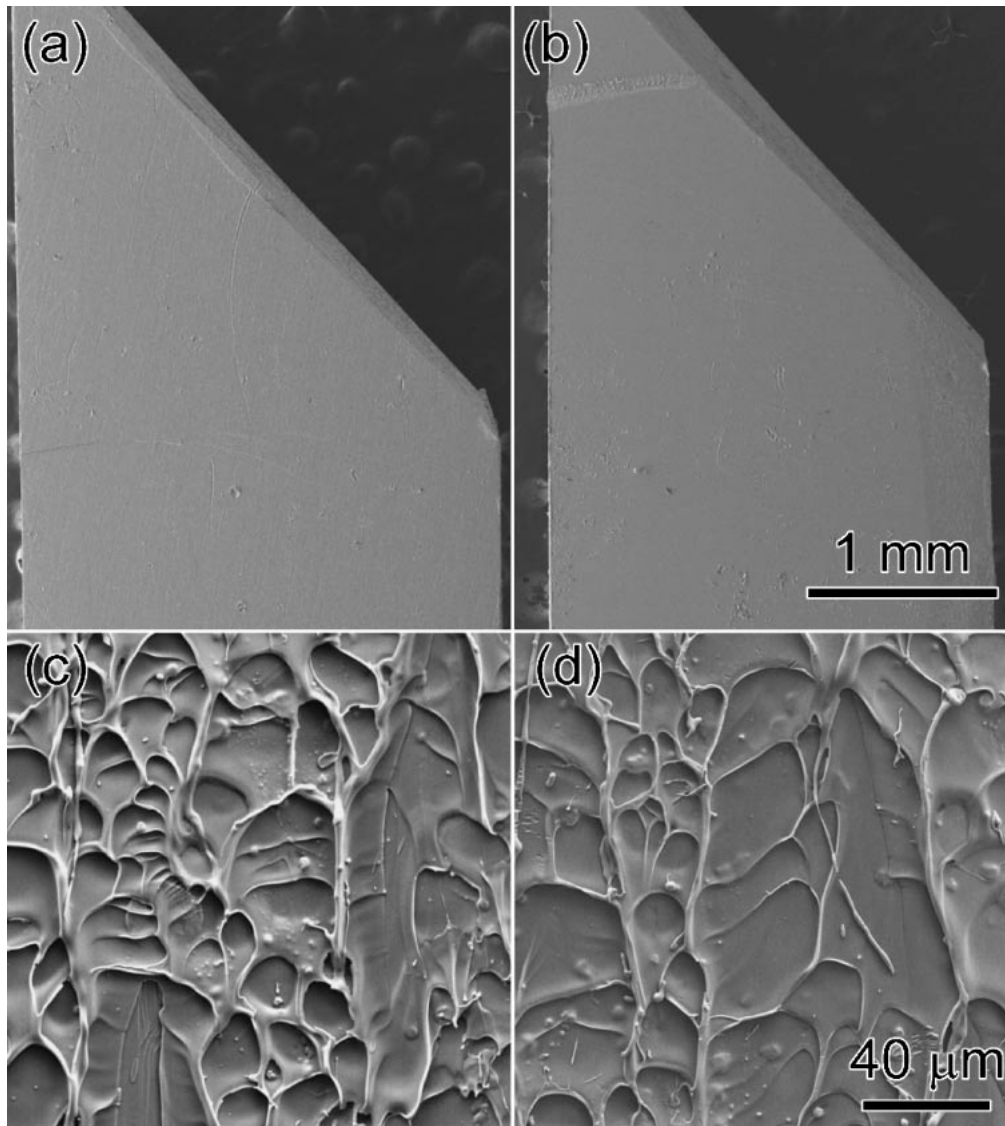


Fig. 9 Fracture surface morphology of the alloy specimens subjected to final fracture under a uniaxial compressive load. Their specimens were taken from the central and surface regions in the transverse cross section taken from the site which is about 15 mm away from the bottom surface of the cast $\text{Zr}_{65}\text{Al}_{7.5}\text{Ni}_{10}\text{Cu}_{17.5}$ alloy rod with a diameter of 16 mm.

interval of about 75 K. The large supercooled liquid region represents that the supercooled liquid has high resistance against crystallization. The high resistance is presumably because the crystallization occurs through the nearly simultaneous precipitation of three crystalline phases, Zr_2Cu , Zr_2Ni and Zr_6NiAl_2 ,^{25,26)} which require the long-range redistribution of the constituent elements. It has been pointed that the redistribution of the constituent elements on a long range scale is rather difficult for the supercooled liquid with fully dense random packing consisting mainly of icosahedral short-range ordered atomic configurations in the quaternary alloy system where the three component rules for stabilization of supercooled liquid are satisfied.^{9,10)} Experimental results and computer simulation have shown that the icosahedral type clusters should be the preferred short-range order (SRO) in metallic glass when the atomic size ratio (R) between solute and solvent atoms is close to 0.85.^{27,28)} This is because the $R \sim 0.85$ is energetically most favored in forming icosahedral clusters.²⁷⁾ For the current $\text{Zr}_{65}\text{Al}_{7.5}\text{Ni}_{10}\text{Cu}_{18.5}$ alloy, $R_{(\text{Cu}/\text{Zr})} = 0.80$, $R_{(\text{Al}/\text{Zr})} = 0.89$,

$R_{(\text{Ni}/\text{Zr})} = 0.78$. As a result, the icosahedral-type SRO should be the main underlying topological SRO in the present $\text{Zr}_{65}\text{Al}_{7.5}\text{Ni}_{10}\text{Cu}_{18.5}$ glassy alloy, which plays an important role in stabilizing the glass configuration.²⁹⁾ Consequently, high stability of the icosahedral-type SRO results in the high stabilization of the supercooled liquid, which is associated with the GFA of the $\text{Zr}_{65}\text{Al}_{7.5}\text{Ni}_{10}\text{Cu}_{18.5}$ glassy alloy. In addition, the high T_g/T_l of 0.55 implies that the viscosity of the supercooled liquid for the present alloy increases rapidly with decreasing temperature, leading to easy solidification of supercooled liquid into a glassy solid state under the suppression of crystallization reaction.

5. Summary

We examined the possibility of producing a bulk glassy alloy rod with useful characteristics in the large diameter range up to 16 mm for $\text{Zr}_{65}\text{Al}_{7.5}\text{Ni}_{10}\text{Cu}_{17.5}$ alloy by the tilt casting method. The results obtained are summarized as follows.

(1) The Zr-based alloy had a critical diameter of at least 16 mm for formation of a glassy phase. The formation of a glassy phase was recognized at the central and outer surface regions in the transverse cross section at the three different sites which were away by about 10 mm, 15 mm and 30 mm from the bottom surface of the cast alloy rod.

(2) The thermal properties of T_g , T_x , T_l and ΔH_x for the samples obtained from the three different sites had nearly the same values, i.e., 643 K, 745 K, 1174 K and 55 to 57 J/g, respectively. The reduced glass transition temperature (T_g/T_l) is also measured to be 0.55. The large ΔT_x and high T_g/T_l are consistent with the large maximum diameter for glass formation.

(3) The Young's modulus, yield strength, elastic strain and plastic strain of the cast glassy alloy rod lie in the narrow range of 85 to 88 GPa, 1540 to 1550 MPa, 0.018 and 0.003 to 0.005, respectively, and are almost independent of sample preparation sites. There was no appreciable change in fracture mode with sample site.

(4) The success of developing a bulk glassy alloy rod exhibiting nearly constant characteristics in the large diameter range up to 16 mm for the Zr-based alloy is promising for future advancement of bulk glassy alloy materials.

Acknowledgements

This work was financially supported by Research and Development Project on Advanced Metallic Glasses, Inorganic Materials and Joining Technology from the Ministry of Education, Culture, Sports, Science and Technology of Japan.

REFERENCES

- 1) A. Inoue, K. Ohtera, K. Kita and T. Masumoto: Japan. J. Appl. Phys. **27** (1988) L2248–2251.
- 2) A. Inoue, T. Zhang and T. Masumoto: Mater. Trans., JIM **30** (1989) 965–972.
- 3) A. Inoue, T. Zhang and T. Masumoto: Mater. Trans., JIM **31** (1990) 177–183.
- 4) A. Inoue and T. Masumoto: Mater. Sci. Eng. A **173** (1993) 1–8.
- 5) A. Inoue, T. Nakamura, T. Sugita, T. Zhang and T. Masumoto: Mater. Trans., JIM **34** (1993) 351–358.
- 6) A. Inoue, T. Zhang, N. Nishiyama, K. Ohba and T. Masumoto: Mater. Trans., JIM **34** (1993) 1234–1237.
- 7) A. Inoue, Y. Yokoyama, Y. Shinohara and T. Masumoto: Mater. Trans., JIM **35** (1994) 923–926.
- 8) A. Inoue: Mater. Trans., JIM **36** (1995) 866–875.
- 9) A. Inoue, T. Zhang and A. Takeuchi: Mater. Sci. Forum **269–272** (1998) 855–864.
- 10) A. Inoue: Acta Mater. **48** (2000) 279–306.
- 11) A. Inoue, T. Zhang and T. Masumoto: J. Non-Cryst. Solids **150** (1992) 396–400.
- 12) A. Inoue and T. Zhang: Mater. Trans., JIM **37** (1996) 185–187.
- 13) A. Inoue, T. Shibata and T. Zhang: Mater. Trans., JIM **36** (1995) 1420–1426.
- 14) X. H. Lin, W. L. Johnson and W. K. Rhim: Mater. Trans., JIM **38** (1997) 473–477.
- 15) A. Gebert, J. Eckert and L. Schultz: Acta Mater. **46** (1998) 5475–5482.
- 16) C. T. Liu, M. F. Chisholm and M. K. Miller: Intermetallics **10** (2002) 1105–1112.
- 17) Y. Yokoyama, E. Mund, A. Inoue and I. Schultz: Mater. Trans. **48** (2007) 3190–3192.
- 18) Y. Yokoyama, T. Yamasaki, P. K. Liaw, R. A. Buchanan and A. Inoue: Mater. Sci. Eng. A **449–451** (2007) 621–626.
- 19) A. Peker and W. L. Johnson: Appl. Phys. Lett. **63** (1993) 2342–2344.
- 20) Q. S. Zhang, W. Zhang and A. Inoue: Mater. Trans. **48** (2007) 629–631.
- 21) Q. S. Zhang, W. Zhang and A. Inoue: Mater. Trans. **48** (2007) 3031–3033.
- 22) J. B. Qiang, W. Zhang, G. Q. Xie and A. Inoue: Appl. Phys. Lett. **90** (2007) 231907-1–3.
- 23) Y. H. Liu, G. Wang, R. J. Wang, D. Q. Zhao, M. X. Pang and W. H. Wang: Science **315** (2007) 1385–1388.
- 24) Y. Yokoyama, T. Yamasaki, M. Nishijima and A. Inoue: Mater. Trans. **48** (2007) 1276–1281.
- 25) J. Saida and A. Inoue: J. Non-Cryst. Solids **312–314** (2002) 502–507.
- 26) J. Saida, M. Matsushita and A. Inoue: Mater. Trans. **43** (2002) 1937–1946.
- 27) H. J. Lee, T. Cagin, W. L. Johnson and W. A. Goddard III: J. Chem. Phys. **119** (2003) 9858–9870.
- 28) H. W. Sheng, W. K. Luo, F. M. Alamgir, J. M. Bai and E. Ma: Nature (London) **439** (2006) 419–425.
- 29) T. Fukunaga, K. Itoh, T. Otomo, K. Mori, M. Sugiyama, H. Kato, M. Hasegawa, A. Hirata, Y. Hirotsu and A. C. Hannon: Intermetallics **14** (2006) 893–897.